

VARs-FL: Validation-Aligned Client Selection for Non-IID Federated Learning in IoT Systems

Mohamed Lakas*, Mohamed Amine Ferrag*[†]

*College of Information Technology, United Arab Emirates University, UAE

[†] Corresponding author: mohamed.ferrag@uaeu.ac.ae

Abstract—Federated learning (FL) systems typically employ stateless client selection, treating each communication round independently and ignoring accumulated evidence of client contribution quality. Under non-IID data, this leads to slow convergence and unstable training, particularly when selection relies on local proxies (e.g., training loss) that are misaligned with the global optimization objective. These challenges are especially pronounced in Internet of Things (IoT) and Industrial IoT (IIoT) environments, where data is highly heterogeneous and distributed across devices observing different traffic patterns. In this paper, we propose VARs-FL (Validation-Aligned Reputation Scoring for Federated Learning), a client selection framework that quantifies each client’s contribution using the reduction in server-side validation loss induced by its update. These per-round signals are aggregated into a Reputation score that combines a sliding-window average of recent contributions with a logarithmically scaled participation term, enabling robust exploration–exploitation selection. VARs-FL requires no changes to local training or aggregation and remains fully compatible with standard FedAvg. We evaluate VARs-FL on a 15-class non-IID IoT intrusion detection task using the Edge-IIoTset dataset with 100 clients across multiple seeds, comparing it against FedAvg, Oort, and Power-of-Choice. VARs-FL consistently improves accuracy, F1-Macro, and loss, while accelerating convergence (up to 36% fewer rounds to reach 80% accuracy). These results demonstrate that validation-aligned, history-aware client selection provides a more reliable and efficient training process for federated learning in heterogeneous IoT environments.

Index Terms—Internet of Things, Federated learning, Non-IID Data, Distributed Learning, Edge Intelligence, Decentralized Optimization

I. INTRODUCTION

Federated learning (FL) enables multiple clients to collaboratively train a shared model without exchanging raw data, making it particularly well-suited for privacy-sensitive environments such as mobile systems and healthcare applications [1], [2]. This paradigm has been successfully deployed in data-distributed scenarios, including mobile keyboard next-word prediction and other forms of on-device personalization, and has gained increasing attention in domains where data sharing is restricted by privacy regulations and policy constraints, such as healthcare and cybersecurity [3].

The Internet of Things (IoT) and Industrial Internet of Things (IIoT) represent especially compelling application domains for FL. These environments comprise large numbers of geographically distributed devices that generate highly heterogeneous, localized data streams. Each node observes only a limited, potentially biased subset of the global data

distribution — e.g., specific traffic patterns or attack types — yet, collectively, these nodes contain the information necessary to train effective intrusion detection systems. However, centralizing such data is often impractical due to bandwidth limitations, data sovereignty requirements, and the sensitive nature of industrial network traffic [4]. In this context, FL provides a principled solution by enabling devices to perform local training and share model updates rather than raw data, thereby enabling collaborative learning while preserving data locality and privacy [5], [6]. A major drawback of FL is the significant communication overhead it introduces. In each round, participating clients upload gradients (or updated model parameters) which can be prohibitively large, particularly for bandwidth-limited clients and deep models [7]. In IIoT environments, edge devices typically operate over constrained wireless links (e.g., LPWAN, narrowband LTE, or shared Wi-Fi), which makes communication overhead a key bottleneck. To mitigate this cost, several complementary approaches have been proposed. First, aggregation and system mechanisms to achieve robust, privacy-preserving updates at scale, e.g., via secure aggregation [8]. Second, update compression to reduce message sizes through quantization and sparsification techniques [7], [9], [10]. Finally, client selection to reduce the number of clients participating per round by scheduling a subset expected to contribute most under resource and data heterogeneity [11], [12].

FedAvg and most standard FL algorithms adopt *stateless* client selection, in which each communication round is treated independently, and selection decisions do not account for historical client behavior. As a result, future participation is not informed by a client’s past contribution to global model improvement [13], [14]. In realistic deployments, client data exhibit significant heterogeneity in quality, quantity, and class distribution, and without tracking past contributions, the FL server cannot distinguish between clients that consistently provide beneficial updates and those that are noisy or uninformative [15], [16]. This limitation is particularly critical in IIoT intrusion detection settings, where the distribution of attack types varies substantially across nodes; for example, a sensor monitoring industrial SCADA traffic may predominantly observe Ransomware and Backdoor attacks, whereas a gateway node may encounter mostly DDoS traffic. Under such non-IID conditions, clients holding rare but important classes are often under-selected despite being essential for improving

global model coverage [17]. This issue is further exacerbated under partial participation: in a federation with 100 clients and a 10% selection rate per round, each client has only a 10% probability of being selected in any given round, regardless of its utility, leading to inefficient training and suboptimal generalization [18].

A further, often underappreciated challenge in federated learning is *objective misalignment*: when client selection is driven by local proxies (e.g., local training loss), the server may over-select clients that optimize their own local objectives while contributing little, or even negatively, to the global objective [19]. This misalignment arises because local loss reflects the client-specific data distribution rather than the global data distribution. Under non-IID conditions, a client holding rare or highly skewed classes may exhibit high local loss not because it is globally informative, but because the current global model is poorly adapted to its distribution. Prioritizing such clients can bias the global model toward their local data, degrading overall generalization [20]. Moreover, this effect accumulates over rounds: repeated selection based on local loss progressively steers the global model into suboptimal directions, thereby degrading the initialization for subsequent updates. Empirically, this phenomenon is evident in methods such as Oort [21], which favor high local-loss clients and consequently exhibit unstable training dynamics, including persistent accuracy oscillations and failure to reach the 80% accuracy threshold within 100 rounds across multiple random seeds [22].

In this paper, we present *VARs-FL*, a client selection framework that simultaneously addresses both the statelessness and objective-misalignment challenges in federated learning, with a particular focus on heterogeneous Internet of Things (IoT) environments, without modifying local training, aggregation, or communication protocols. Unlike prior approaches that rely on local proxies, *VARs-FL* directly measures each client’s contribution using server-side validation loss, providing a signal that is inherently aligned with the global optimization objective. This validation-driven signal identifies clients that contribute to global generalization, requires no additional client-side disclosures beyond model updates, and is accumulated over time into a per-client *Reputation* score that captures consistent contribution across rounds.

The main contributions of this paper are as follows:

- (i) We propose a *validation-loss-based quality score* that directly quantifies each client’s per-round contribution to global model improvement using a server-side validation set, ensuring alignment with the global objective by construction, particularly under non-IID data distributions common in IoT systems;
- (ii) We introduce a *Reputation scoring mechanism* that combines a sliding-window average of recent quality scores with a logarithmically scaled participation term, enabling selection decisions to prioritize consistent contribution rather than mere participation frequency in dynamic and heterogeneous IoT environments;

- (iii) We develop a *multi-armed bandit (MAB)-based selection strategy* that formulates client selection as an explore–exploit problem, balancing the discovery of informative clients with the repeated selection of those that have demonstrated reliable global benefit in non-stationary IoT settings;
- (iv) We conduct an extensive evaluation of *VARs-FL* on the Edge-IIoTset Cyber Security Dataset [3] in a 100-client, non-IID IoT intrusion detection setting across multiple random seeds.

The remainder of this paper is organized as follows. Section II reviews related work on federated learning under data heterogeneity, client selection strategies, reputation and trust mechanisms, bandit-based optimization, and FL-based intrusion detection. Section III presents the *VARs-FL* framework, including data preprocessing, model architecture, validation-loss-based quality scoring, reputation aggregation, the explore–exploit selection policy, and complexity analysis. Section IV describes the experimental setup, including the dataset, non-IID partitioning scheme, baselines, and evaluation metrics. Section V reports and analyzes the experimental results in terms of overall performance, convergence speed, training dynamics, and per-class recall. Finally, Section VI concludes the paper and outlines directions for future work.

II. RELATED WORK

This section reviews prior work relevant to *VARs-FL* across five complementary directions. We first discuss approaches that address data heterogeneity in federated learning, focusing on optimization-based methods that mitigate client drift. Then, we examine existing client selection strategies and highlight their reliance on local proxy signals. Next, we review reputation and trust mechanisms, followed by bandit-based formulations for adaptive client selection. Finally, we cover applications of federated learning in IoT security and intrusion detection. Throughout, we emphasize the gap between local utility estimation and global objective alignment, which motivates the design of *VARs-FL*.

A. Federated Learning Under Data Heterogeneity

Data heterogeneity is a fundamental challenge in federated learning. In realistic deployments, client data distributions differ in label composition, feature space, and sample volume, a setting commonly referred to as non-IID (non-independent and identically distributed). Li et al. [28] show that such heterogeneity induces *client drift*, where local updates move the global model toward client-specific optima, thereby degrading global generalization and slowing convergence even under standard FedAvg [1].

Several approaches mitigate client drift by modifying the local optimization objective. FedProx [23] introduces a proximal term to limit deviation from the global model. SCAF-FOLD [29] employs control variates to correct gradient drift, while MOON [30] leverages contrastive learning to align local and global representations. Although these methods reduce the adverse effects of heterogeneous updates, they do not address

TABLE I
COMPARISON OF CLIENT SELECTION METHODS ACROSS KEY DESIGN DIMENSIONS

Method	Utility Signal	History Aware	Global Alignment	Non-IID Robustness	Minority Support	IoT/Sec. Eval.
FedAvg [1]	None	No	–	No	No	No
FedProx [23]	None	No	–	Partial	No	No
PoC [24]	Local loss	No	Indirect	Partial	No	No
Oort [21]	Local loss	No	Indirect	No	No	No
Active FL [25]	Grad. norm	No	Partial	No	No	No
FedCor [26]	Grad. corr.	No	Partial	Partial	No	No
FLTrust [27]	Cosine sim.	No	Partial	Partial	No	No
VARs-FL (Ours)	Val. loss	Yes	Explicit	Yes	Yes	Yes

Utility Signal: metric used to estimate client contribution (e.g., validation loss, gradient norm). *History Aware*: whether past client performance is incorporated. *Global Alignment*: whether the signal directly reflects improvement in the global objective. *Non-IID Robustness*: reported stability under heterogeneous data distributions. *Minority Support*: explicit consideration of rare or underrepresented classes. *IoT/Sec. Eval.*: evaluation on IoT or cybersecurity datasets.

client selection; instead, they assume uniform participation and focus on stabilizing the optimization process. VARs-FL is complementary to these approaches. Rather than mitigating the impact of arbitrary client selection, VARs-FL reduces the likelihood of selecting clients whose updates are misaligned with the global objective. As such, it operates at the selection stage, orthogonal to optimization-based methods, and can be integrated with techniques such as FedProx or SCAFFOLD without modification.

B. Client Selection Strategies

Client selection plays a critical role in federated learning, particularly under heterogeneous data distributions. Standard FedAvg [1] selects clients uniformly at random, ignoring both update quality and data distribution, which leads to statistical inefficiency. For instance, in a federation with 100 clients and a 10% participation rate, a client holding rare but important data has only a 10% probability of being selected in any round, regardless of its utility. Prior work propose various strategies to estimate client utility, typically using local proxies. Power-of-Choice [24] prioritizes clients with high local loss, assuming they contain under-learned data. However, this conflates local difficulty with global utility, as high local loss may arise from distributional divergence rather than informative content. Active federated learning [25] uses gradient norms as a proxy for informativeness, while FedCor [26] models inter-client loss correlations via Gaussian processes to guide selection.

Oort [21] combines statistical utility and system efficiency, using local loss as the utility signal, while FedScale [31] extends this paradigm to large-scale system-aware benchmarking. FedCS [11] focuses on resource-constrained environments, selecting clients based on latency constraints [12].

A fundamental limitation of these methods is their reliance on *local proxies*—such as local loss, gradient norm, or correlation—as surrogates for global utility. These signals reflect properties of local data distributions rather than the actual contribution to the global objective. Under non-IID settings, prioritizing such proxies can degrade global performance. VARs-FL addresses this limitation by replacing local

proxies with a direct, server-side measurement of each client’s contribution via validation-loss reduction.

C. Reputation and Trust Mechanisms in Federated Learning

Several works address robustness in federated learning, particularly under adversarial settings. Krum [32] and its extension Multi-Krum select updates that are closest to their neighbors in parameter space, filtering out potential Byzantine clients. Bulyan [33] further improves robustness by combining neighbor-based filtering with coordinate-wise median aggregation. FLTrust [27] introduces a server-side trusted dataset to compute a reference gradient, scoring client updates based on cosine similarity. Updates that deviate from the trusted direction are down-weighted or discarded, providing robustness against malicious participants. However, FLTrust is designed for adversarial settings and evaluates directional similarity rather than contribution to global generalization. In contrast, VARs-FL assumes honest but heterogeneous clients and focuses on measuring contribution to the global objective. It uses validation-loss reduction as a scoring signal and accumulates this signal over time into a reputation score, whereas FLTrust operates on a per-round basis without temporal aggregation. Personalized FL methods, such as FedRep [34] and pFedMe [35], maintain per-client model components tailored to local data. While these approaches capture client-specific characteristics, they do not leverage this information for global client selection. To our knowledge, VARs-FL is the first framework to explicitly maintain a temporally aggregated, validation-aligned reputation score for client selection.

D. Bandit-Based Optimisation for Client Selection

Client selection can be naturally formulated as a multi-armed bandit (MAB) problem [21], [24], where each client represents an arm and the objective is to balance exploration and exploitation. Oort [21] employs an upper-confidence-bound-like strategy combining utility and system efficiency. However, existing bandit-based approaches rely on local proxy signals that are misaligned with the global objective. VARs-FL

addresses this limitation by defining the reward as validation-loss reduction, aligning the bandit objective with the global training objective. The resulting reputation score R_i^t can be interpreted as a non-stationary bandit estimator [36], combining short-term quality estimates with long-term participation. Thompson Sampling [37] provides a Bayesian alternative with strong theoretical guarantees in stationary settings. However, federated learning is inherently non-stationary, as the global model evolves over time. Prior work [36] shows that sliding-window or discounted approaches are necessary in such settings. VARS-FL incorporates this insight through a sliding-window quality estimator, enabling adaptation to changing client utility.

E. Federated Learning for IoT Security and Intrusion Detection

Federated learning is particularly well-suited to IoT and IIoT environments, where data is distributed, sensitive, and difficult to centralize [38]. In this context, FL enables collaborative intrusion detection without exposing raw network traffic. Several FL-based intrusion detection systems (FL-IDS) have been proposed. D²IoT [39] learns device-specific behavioral models across distributed gateways, achieving high detection performance. Rey et al. [40] demonstrate that FL achieves performance comparable to centralized training while improving robustness through data diversity, although they also highlight vulnerability to poisoning attacks. Rahman et al. [41] show that FL outperforms local models and approaches centralized performance under heterogeneous data distributions. Common benchmark datasets include CICIDS2017 [42], ToN-IoT [43], and N-BaIoT [44]. However, these datasets have limitations in realism or scope. Edge-IIoTset [3] provides a more comprehensive benchmark, with over 2.2 million samples across 15 classes, including rare attack types and significant class imbalance, making it well-suited for evaluating client selection under non-IID conditions. Despite these advances, existing FL-IDS works primarily rely on FedAvg or simple selection schemes and do not address objective misalignment. VARS-FL fills this gap by providing a validation-aligned client selection mechanism tailored to heterogeneous IoT environments.

F. Summary and Positioning

Table I summarizes the key design dimensions of existing client selection and related federated learning methods. A clear pattern emerges: most approaches rely on *local proxy signals* (e.g., local loss, gradient norms, or correlations) that are not inherently aligned with the global optimization objective, and are therefore unreliable under heterogeneous (non-IID) data distributions. In addition, existing methods are largely *stateless*, treating each round independently and failing to accumulate evidence about a client’s historical contribution. While some works address system heterogeneity or adversarial robustness, none simultaneously tackle *objective misalignment* and *data heterogeneity*, nor do they evaluate client selection in realistic IoT and cybersecurity settings characterized by severe class imbalance and distributed data. VARS-FL addresses these

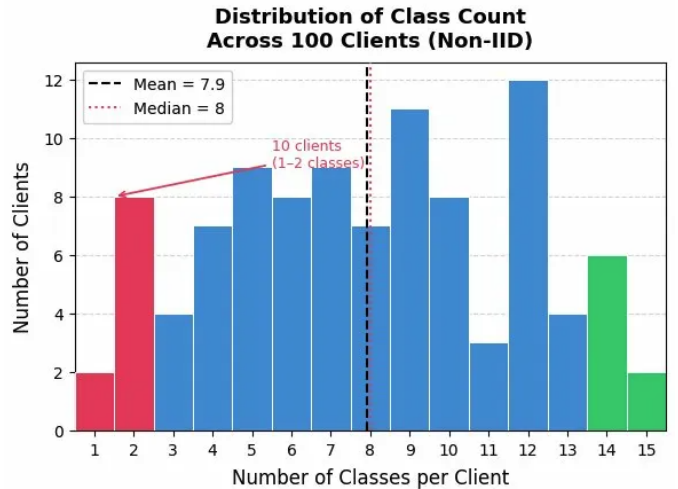


Fig. 1. Non-IID class presence across 100 clients (seed 42). Each row is a client sorted by class count; each column is an attack class. White indicates absence. Dataset sizes range from 426 to 5,152 samples per client (mean: 3,250); the number of local classes ranges from 1 to 15 (mean: 7.9), reflecting the heterogeneous data distributions characteristic of real IoT deployments.

limitations through a unified framework that (i) defines client utility via a *globally aligned* validation-loss reduction signal, (ii) maintains a *history-aware reputation score* that aggregates per-client contributions across rounds, and (iii) employs an *explore-exploit selection strategy* to balance discovery and exploitation under non-stationary conditions. To the best of our knowledge, VARS-FL is the first method to combine these three properties within a single framework while remaining fully compatible with standard federated learning pipelines, thereby providing a principled and practical solution for client selection in real-world non-IID and IoT-driven environments.

III. SYSTEM MODEL

Figure 2 provides an overview of VARS-FL, where client selection is driven by validation-aligned contribution signals and accumulated reputation, enabling objective-consistent and history-aware participation under non-IID data. Specifically, VARS-FL consists of two types of participants. The **server** coordinates the training process, maintains the global model θ , holds a shared validation set, and tracks all client-level statistics. The **clients** ($\mathcal{C} = \{1, \dots, N\}$) retain their local datasets \mathcal{D}_i and perform training locally, returning updated model parameters to the server without exposing raw data. Table II summarizes the notation used throughout this section, providing definitions for all variables, parameters, and symbols employed in the formulation of the VARS-FL framework.

Each communication round t proceeds as follows:

- 1) The server selects a subset $S_t \subseteq \mathcal{C}$ with $|S_t| = m$ and broadcasts the current global model θ^{t-1} .
- 2) Each client $i \in S_t$ trains locally on \mathcal{D}_i for E epochs and returns updated parameters θ_i^t .
- 3) The server evaluates each client’s contribution via a quality score Q_i^t and updates its Reputation score R_i^t .
- 4) The server aggregates the updates using standard FedAvg:

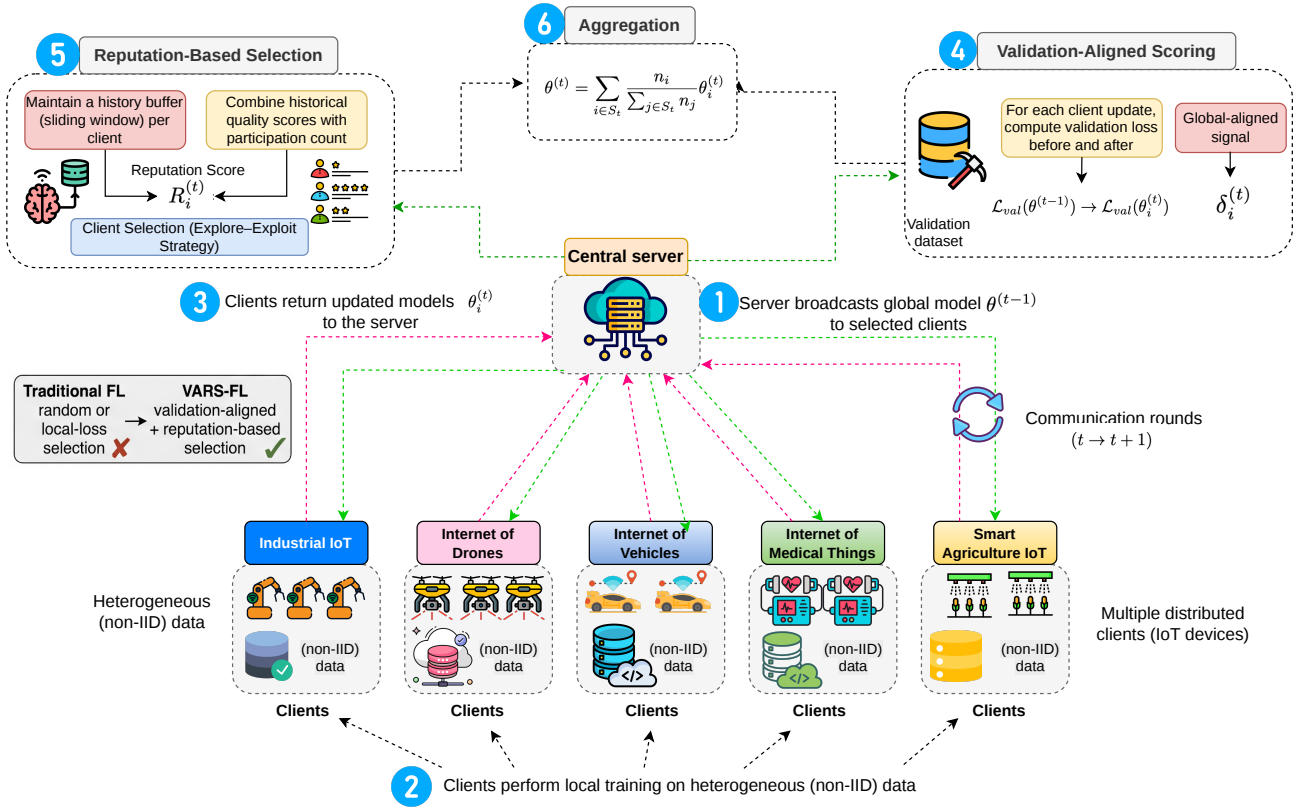


Fig. 2. Overview of **VARS-FL**, a validation-aligned, reputation-based client selection framework for federated learning. In each communication round, the server broadcasts the global model to selected clients, which perform local training on heterogeneous (non-IID) data and return updated models. The server evaluates each client’s contribution using validation-loss improvement, producing a globally aligned quality signal that is aggregated over time into a reputation score. Client selection is then performed using an explore-exploit strategy based on these reputation scores, while aggregation remains unchanged via FedAvg.

$$\theta^t = \sum_{i \in S_t} \frac{n_i}{\sum_{j \in S_t} n_j} \theta_i^t, \quad (1)$$

where n_i denotes the number of local samples held by client i . Reputation scores influence *client selection* in subsequent rounds but are not used as aggregation weights, ensuring full compatibility with the standard FedAvg protocol.

A. Data Preprocessing

The Edge-IIoTset dataset contains 63 raw features, of which 19 correspond to non-numeric protocol fields—including IP address strings, HTTP URI components, MQTT payload content, and TCP port identifiers—that lack a meaningful ordinal structure for gradient-based learning. These features are removed, resulting in a 43-dimensional numeric feature space. The retained features capture packet-level statistics, flow-level counters, and protocol-specific attributes across TCP, UDP, DNS, HTTP, MQTT, and ARP layers. No further feature selection or dimensionality reduction is applied in order to preserve the full set of available numerical signals.

To mitigate class imbalance, the majority class (*Normal*) is capped at 18% of the total sample count. In the original dataset, Normal traffic accounts for 1,615,643 out of 2,219,201

samples (72.8%); after capping, it is reduced to 132,488 samples, yielding a balanced dataset of 736,046 samples across 15 classes. This strategy prevents the model from collapsing to a majority-class predictor while preserving a realistic distribution of attack categories. All features are standardized to zero mean and unit variance using statistics computed on the training set, and the same transformation is applied to validation and test splits to avoid data leakage.

The dataset is partitioned into training, validation, and test sets using a 70/15/15 split, corresponding to 515,232, 110,407, and 110,407 samples, respectively. The validation set is maintained exclusively at the server and is used solely for client quality evaluation (Eq. 7); it is neither shared with clients nor used for gradient updates. Training data is distributed across clients using a heterogeneous non-IID partitioning scheme. Client dataset sizes range from 426 to 5,152 samples (mean: 3,250), and the number of classes per client varies from 1 to 15 (mean: 7.9, median: 8). This results in a highly heterogeneous distribution, where some clients observe only a single attack type while others cover the full class space, reflecting the diversity of real-world IoT deployments. The resulting non-IID structure is illustrated in Fig. 1.

TABLE II
SUMMARY OF NOTATION USED IN THE SYSTEM MODEL

Symbol	Description
\mathcal{C}	Set of all clients
N	Total number of clients
i	Client index
t	Communication round index
S_t	Set of selected clients at round t
m	Number of clients selected per round
\mathcal{D}_i	Local dataset of client i
n_i	Number of samples at client i
\mathcal{D}_{val}	Server-side validation dataset
θ	Global model parameters
θ^t	Global model at round t
θ_i^t	Local model returned by client i at round t
E	Number of local training epochs
$\mathcal{L}_{val}(\cdot)$	Validation loss function
δ_i^t	Validation-loss improvement of client i
Q_i^t	Quality score of client i at round t
H_i	History of past quality scores for client i
$\bar{Q}_i^{(t)}$	Sliding-window average of recent quality scores
R_i^t	Reputation score of client i at round t
p_i^t	Participation count of client i
W	Sliding-window size for quality averaging
ε	Minimum floor value for normalized quality score
ζ	Small constant for numerical stability
ρ	Exploration rate in client selection
T_0	Number of cold-start rounds
w	Global model (algorithm notation)
w_i	Local model returned by client i (algorithm notation)
C_{fwd}	Forward-pass computational cost per sample
ΔC_{server}	Additional server-side computation per round
d_k	Dimension of layer k in the neural network
\mathbf{x}	Input feature vector
\mathbf{h}_k	Hidden layer representation at layer k
\mathbf{z}_k	Post-dropout activation at layer k
$\hat{\mathbf{y}}$	Predicted output probability vector
$\mathbf{W}_k, \mathbf{b}_k$	Weight matrix and bias vector of layer k

B. Model Architecture

VARS-FL is model-agnostic by design: the server-side quality scoring mechanism evaluates the validation loss of any model returned by clients, independent of architecture or parameterization. In this work, we instantiate VARS-FL using a fully connected deep neural network (DNN), a compact and interpretable architecture well-suited for tabular network traffic data.

Input representation. Each sample is represented as a 43-dimensional real-valued vector $\mathbf{x} \in \mathbb{R}^{43}$, corresponding to the standardized numeric features.

Hidden layers. The network consists of three fully connected layers with decreasing width and ReLU activations:

$$\mathbf{h}_1 = \text{ReLU}(\mathbf{W}_1 \mathbf{x} + \mathbf{b}_1), \quad \mathbf{W}_1 \in \mathbb{R}^{128 \times 43}, \quad (2)$$

$$\mathbf{h}_2 = \text{ReLU}(\mathbf{W}_2 \mathbf{z}_1 + \mathbf{b}_2), \quad \mathbf{W}_2 \in \mathbb{R}^{64 \times 128}, \quad (3)$$

$$\mathbf{h}_3 = \text{ReLU}(\mathbf{W}_3 \mathbf{z}_2 + \mathbf{b}_3), \quad \mathbf{W}_3 \in \mathbb{R}^{32 \times 64}, \quad (4)$$

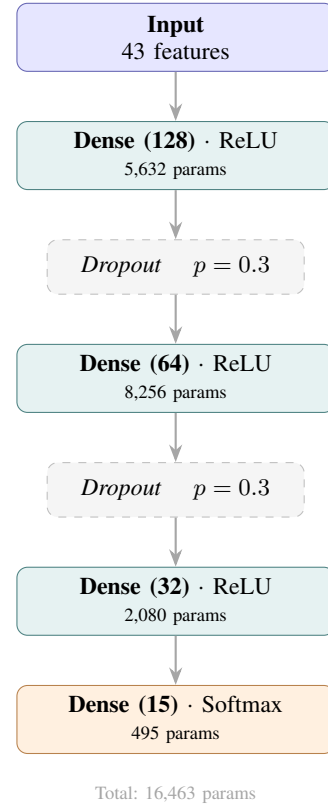


Fig. 3. Architecture of the fully connected DNN used in the federated learning experiments. The model takes 43 standardized numeric features as input, followed by three hidden layers of sizes 128, 64, and 32 with ReLU activations. Dropout ($p = 0.3$) is applied after the first two hidden layers, and the output layer uses softmax activation for multi-class classification.

where $\mathbf{z}_1 = \text{Dropout}(\mathbf{h}_1, p = 0.3)$ and $\mathbf{z}_2 = \text{Dropout}(\mathbf{h}_2, p = 0.3)$. Dropout is applied during training to mitigate overfitting under heterogeneous client data distributions and is disabled at inference time.

Output layer. A linear projection followed by softmax produces class probabilities over the 15 traffic classes:

$$\hat{\mathbf{y}} = \text{softmax}(\mathbf{W}_4 \mathbf{h}_3 + \mathbf{b}_4), \quad \mathbf{W}_4 \in \mathbb{R}^{15 \times 32}. \quad (5)$$

Model size. The total number of trainable parameters is:

$$\begin{aligned} |\theta| &= (43 \cdot 128 + 128) + (128 \cdot 64 + 64) \\ &\quad + (64 \cdot 32 + 32) + (32 \cdot 15 + 15) \\ &= 16,463. \end{aligned} \quad (6)$$

This compact design reduces communication overhead, which is critical in bandwidth-constrained federated environments.

Training configuration. The model is trained using the Adam optimizer with learning rate $\eta = 10^{-3}$ and categorical cross-entropy loss. Federated hyperparameters are summarized in Table IV.

C. Validation-Loss Improvement

At the end of each round, the server assigns a quality score $Q_i^t \in [0, 1]$ to each participating client, reflecting its

Algorithm 1 VARS-FL Training Procedure

Require: Clients $\mathcal{C} = \{1, \dots, N\}$, rounds T , clients per round m , validation set \mathcal{D}_{val} , initial model w_0

- 1: Initialize global model $w \leftarrow w_0$
- 2: **for all** clients $i \in \mathcal{C}$ **do**
- 3: Initialize participation count $p_i \leftarrow 0$
- 4: Initialize quality history $H_i \leftarrow []$
- 5: **end for**
- 6: **for** $t = 1$ **to** T **do**
- 7: Select clients S_t using Algorithm 2
- 8: **for all** clients $i \in S_t$ **do**
- 9: Send w to client i
- 10: Client trains locally and returns updated model w_i and sample count n_i
- 11: **end for**
- 12: Update client quality histories and participation counts using Algorithm 3
- 13: Aggregate updates using FedAvg:
- 14: $w \leftarrow \sum_{i \in S_t} \frac{n_i}{\sum_{j \in S_t} n_j} w_i$
- 15: **end for**
- 16: **return** w

contribution to global model improvement as measured on the server-side validation set.

To compute this signal, the server evaluates the validation loss before and after applying each client’s update. The validation-loss improvement is defined as:

$$\delta_i^t = \max(0, \mathcal{L}_{val}(\theta^{t-1}) - \mathcal{L}_{val}(\theta_i^t)), \quad (7)$$

where θ_i^t denotes the model obtained by applying client i ’s update. Updates that degrade validation performance receive $\delta_i^t = 0$.

To enable relative comparison within a round, the scores are normalized:

$$Q_i^t = \max\left(\varepsilon, \frac{\delta_i^t}{\max_{j \in S_t} \delta_j^t + \zeta}\right), \quad (8)$$

where $\varepsilon > 0$ is a small floor value and ζ ensures numerical stability. This normalization emphasizes relative contribution and prevents dominance by a single client, while ε ensures continued exploration.

D. From Quality Scores to Reputation

Single-round quality scores can be noisy; therefore, VARS-FL aggregates evidence over time through a *Reputation* score. For each client, we maintain a sliding-window average $\bar{Q}_i^{(t)}$ over the most recent W scores and a participation count p_i^t . The reputation is defined as:

$$R_i^t = \bar{Q}_i^{(t)} \cdot \log(1 + p_i^t), \quad (9)$$

where $W = 5$ in our experiments. The logarithmic term provides diminishing returns for frequent participation, ensuring that consistent quality—rather than frequency alone—drives selection priority.

Algorithm 2 Reputation-Based Client Selection

Require: Clients \mathcal{C} , histories $\{H_i\}$, participation counts $\{p_i\}$, clients per round m , exploration rate ρ , cold-start rounds T_0 , current round t

- 1: **for all** clients $i \in \mathcal{C}$ **do**
- 2: **if** $|H_i| > 0$ **then**
- 3: $\bar{Q}_i \leftarrow \frac{1}{|H_i|} \sum_{q \in H_i} q$
- 4: $R_i \leftarrow \bar{Q}_i \cdot \log(1 + p_i)$
- 5: **else**
- 6: $R_i \leftarrow 0$
- 7: **end if**
- 8: **end for**
- 9: **if** $t \leq T_0$ **then**
- 10: Sample $S_t \subset \mathcal{C}$ uniformly at random such that $|S_t| = m$
- 11: **else**
- 12: $m_{rep} \leftarrow \lfloor (1 - \rho)m \rfloor$
- 13: $m_{rnd} \leftarrow m - m_{rep}$
- 14: $S_t^{rep} \leftarrow$ top- m_{rep} clients according to R_i
- 15: Sample $S_t^{rnd} \subset \mathcal{C} \setminus S_t^{rep}$ uniformly at random such that $|S_t^{rnd}| = m_{rnd}$
- 16: $S_t \leftarrow S_t^{rep} \cup S_t^{rnd}$
- 17: **end if**
- 18: **return** S_t

E. Explore–Exploit Selection

Client selection is formulated as a multi-armed bandit (MAB) problem, where each client represents an arm and rewards are observed only upon selection. In VARS-FL, the reward corresponds to the validation-aligned quality score Q_i^t , and the objective is to maximize cumulative validation-loss reduction under a budget of m clients per round.

We adopt a hybrid explore–exploit strategy: a majority of clients are selected based on the highest reputation scores (exploitation), while the remaining slots are filled via uniform random sampling (exploration). This approach ensures that potentially informative clients are not permanently excluded, while prioritizing those with demonstrated utility. The resulting policy is robust to both non-IID data and non-stationary client contributions.

The overall VARS-FL procedure is decomposed into three components: (i) the main federated training loop (Algorithm 1), (ii) reputation-based client selection (Algorithm 2), and (iii) validation-aligned quality scoring (Algorithm 3). This modular decomposition highlights the separation between standard federated optimization and the proposed selection and scoring mechanisms.

F. Computational and Communication Complexity

Communication overhead. In each round, every selected client uploads a full copy of the model parameters θ_i^t to the server. For the DNN used in this work, this corresponds to $|\theta| = 16,463$ parameters, i.e., $16,463 \times 32 = 526,816$ bits (≈ 64 KB) per client per round under 32-bit floating-point representation. For m participating clients, the total uplink communication per round is therefore $m \cdot 64$ KB.

Algorithm 3 Validation-Aligned Quality Scoring

Require: Selected clients S_t , global model w , returned models $\{w_i\}_{i \in S_t}$, validation set \mathcal{D}_{val} , histories $\{H_i\}$, participation counts $\{p_i\}$, window size W

- 1: $L_{base} \leftarrow \mathcal{L}_{val}(w; \mathcal{D}_{val})$
 - 2: **for all** clients $i \in S_t$ **do**
 - 3: $L_i \leftarrow \mathcal{L}_{val}(w_i; \mathcal{D}_{val})$
 - 4: $\delta_i \leftarrow \max(0, L_{base} - L_i)$
 - 5: **end for**
 - 6: $\delta_{max} \leftarrow \max_{j \in S_t} \delta_j$
 - 7: **for all** clients $i \in S_t$ **do**
 - 8: $Q_i \leftarrow \max\left(\varepsilon, \frac{\delta_i}{\delta_{max} + \zeta}\right)$
 - 9: Append Q_i to H_i
 - 10: **if** $|H_i| > W$ **then**
 - 11: Remove the oldest element from H_i
 - 12: **end if**
 - 13: $p_i \leftarrow p_i + 1$
 - 14: **end for**
 - 15: **return** Updated $\{H_i\}$ and $\{p_i\}$
-

Importantly, VARS-FL introduces *no additional communication overhead* beyond standard FedAvg (Algorithm 1). Clients transmit only model updates and do not report any auxiliary statistics. All additional computations associated with client selection and scoring (Algorithms 2 and 3) are performed entirely on the server. Consequently, VARS-FL maintains identical communication cost to FedAvg and incurs strictly lower overhead than methods that require extra client-side information, such as local loss (Oort, Power-of-Choice) or full gradients (FedCor).

Server-side overhead. The additional computational cost of VARS-FL arises from validation-based client scoring (Algorithm 3). For each selected client, the server performs a forward pass of the returned model θ_i^t over the validation set \mathcal{D}_{val} to compute $\mathcal{L}_{val}(\theta_i^t)$. This operation involves only inference (no gradient computation) and is fully parallelizable across clients.

The per-sample forward-pass cost of the DNN is:

$$\begin{aligned} C_{fwd} &= \sum_k d_{k-1} d_k \\ &= 43 \cdot 128 + 128 \cdot 64 + 64 \cdot 32 + 32 \cdot 15 \\ &= 16,224 \text{ MACs,} \end{aligned} \quad (10)$$

where MAC denotes a multiply-accumulate operation and d_k is the dimension of layer k . The total additional server-side cost per round is:

$$\Delta C_{server} = m \cdot |\mathcal{D}_{val}| \cdot C_{fwd}. \quad (11)$$

For our configuration ($m = 10$, $|\mathcal{D}_{val}| = 110,407$), this yields approximately 1.79×10^{10} MACs per round. Since inference is significantly cheaper than training and can be parallelized, this overhead remains modest compared to the cumulative cost of local training across clients.

Scalability. A key property of VARS-FL is that its additional computational cost depends only on the number of selected clients m and the validation set size $|\mathcal{D}_{val}|$, but is *independent of the total number of clients* N . As a result, the overhead remains constant as the federation scales, making VARS-FL well-suited for large-scale deployments. This contrasts with methods such as FedCor, whose complexity scales as $\mathcal{O}(m^2 \cdot |\theta|)$ due to pairwise client interactions.

Memory overhead. VARS-FL maintains a history buffer of size W for each client, resulting in a total storage cost of $\mathcal{O}(N \cdot W)$ scalar values on the server (Algorithm 2). In practice, this overhead is negligible; for $N = 100$ and $W = 5$, it corresponds to only 500 floating-point values.

Table III summarizes the communication and computational complexity of all compared methods.

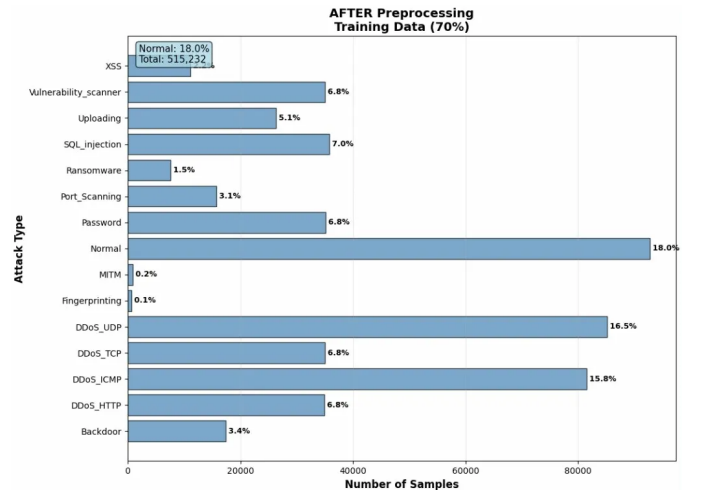


Fig. 4. Class distribution of the training split (515,232 samples) after preprocessing. Normal is capped at 18% to prevent majority-class dominance. MITM (0.2%), Fingerprinting (0.1%), and Ransomware (1.5%) are the rarest classes; validation and test splits share identical proportions, confirming the server validation set is representative of the test distribution.

IV. EXPERIMENTAL SETUP

A. Dataset and Non-IID Data Partitioning

We evaluate VARS-FL on the Edge-IIoTset Cyber Security Dataset [3], a large-scale and realistic IoT/IIoT network traffic benchmark comprising 2,219,201 samples with 63 raw features and 15 traffic classes. These include one benign class (*Normal*) and 14 attack categories, such as Ransomware, SQL injection, multiple DDoS variants (HTTP, TCP, UDP, ICMP), MITM, XSS, Backdoor, Port Scanning, Vulnerability Scanner, Uploading, Fingerprinting, and Password attacks.

The dataset is partitioned into training, validation, and test sets using a 70/15/15 split, corresponding to 515,232, 110,407, and 110,407 samples, respectively. The validation set is maintained exclusively at the server and is used solely for client quality evaluation via δ_i^t (Eq. 7); it is not used for model training.

To reflect realistic deployment conditions, the training data is distributed across clients using a heterogeneous non-IID

TABLE III
COMPLEXITY COMPARISON OF CLIENT SELECTION METHODS

Method	Extra Client Comm.	Server Cost	State
FedAvg [1]	None	None	None
PoC [24]	Loss scalar	$\mathcal{O}(1)$ per client	None
Oort [21]	Loss scalar	$\mathcal{O}(1)$ per client	None
FedCor [26]	Full gradient ($ \theta $)	$\mathcal{O}(m^2 \cdot \theta)$	None
VARs-FL (Ours)	None	$\mathcal{O}(m \cdot \mathcal{D}_{val} \cdot C_{fwd})$	$\mathcal{O}(N \cdot W)$

TABLE IV
EXPERIMENTAL CONFIGURATION

Item	Setting
Rounds	$T = 100$
Clients per round	$m = 10\%$
Local epochs	$E = 3$
Optimizer	Adam
Learning rate	$\eta = 10^{-3}$
Batch size	256
Baselines	FedAvg, Oort, Power-of-Choice
Seeds (robustness)	7, 42, 123
VARs-FL hyperparameters	$T_0 = 15, \rho = 0.3, W = 5$

partitioning scheme. This setup captures the variability inherent in IoT environments, where individual nodes observe different traffic patterns and attack types. In the 100-client setting, local dataset sizes range from 426 to 5,152 samples (mean: 3,250), and the number of classes per client varies from 1 to 15. This results in a highly skewed distribution, where some clients contain only a single attack type while others observe a broader spectrum of traffic, as illustrated in Fig. 4.

B. Models and Configurations

We compare VARs-FL against three representative client selection baselines: *FedAvg* [1], *Oort* [21], and *Power-of-Choice* [24]. To ensure a fair comparison, all methods use the same model architecture, optimizer, learning rate, number of local epochs, and aggregation rule (FedAvg). This isolates the effect of client selection from other factors.

The experimental configuration is summarized in Table IV. We run all experiments for $T = 100$ communication rounds with a participation rate of $m = 10\%$ per round. Local training is performed for $E = 3$ epochs using the Adam optimizer with learning rate $\eta = 10^{-3}$ and batch size 256. To evaluate robustness, results are averaged across three random seeds (7, 42, and 123). VARs-FL-specific hyperparameters are set to $T_0 = 15$ (cold-start rounds), $\rho = 0.3$ (exploration rate), and $W = 5$ (reputation window size).

C. Evaluation Metrics

We evaluate performance using test-set accuracy, macro-averaged F1 score (F1-Macro), weighted F1 score, and cross-entropy loss. Among these, F1-Macro is the primary metric, as it assigns equal importance to all classes and therefore

provides a more informative assessment under class imbalance. This is particularly important in intrusion detection scenarios, where rare attack types must be detected reliably despite their low frequency.

V. RESULTS

A. Overall Performance

This section evaluates whether VARs-FL provides measurable gains over established client-selection strategies. We run experiments with $N = 100$ clients over $T = 100$ communication rounds, comparing VARs-FL against FedAvg (baseline), Oort, and Power-of-Choice, while keeping the model architecture, optimizer, and FedAvg aggregation fixed across methods. Evaluation is done on a held-out test set using accuracy, F1-Macro, weighted F1, and cross-entropy loss, with experiments repeated across multiple random seeds to assess both average performance and robustness.

Table V aggregates results over three random seeds (7, 42, and 123) and shows that VARs-FL achieves the best mean performance on every metric while also having strong consistency across runs. VARs-FL attains the highest mean Accuracy (0.8185 ± 0.0040), F1-Macro (0.6422 ± 0.0241), F1-Weighted (0.8086 ± 0.0080), and Precision (0.8026 ± 0.0392), and the lowest mean Loss (0.4937 ± 0.0200). Relative to FedAvg, VARs-FL delivers consistent gains of $+0.0514$ Accuracy, $+0.0857$ F1-Macro, and $+0.0584$ F1-Weighted, while reducing Loss by -0.0916 . Notably, VARs-FL’s very small standard deviations for Accuracy and F1-Weighted indicate that its advantage is not driven by a single favorable initialization, but persists reliably across seeds.

Looking beyond average performance gains, the observed pattern of improvement reveals where VARs-FL provides the most practical value. The most significant improvement is observed in F1-Macro, which is sensitive to class imbalance and minority class behavior; the $+0.0857$ mean increase over FedAvg suggests VARs-FL improves class balanced generalization rather than simply optimizing dominant class accuracy. In parallel, the substantial Loss reduction implies more stable convergence and better validation-aligned updates, consistent with selecting clients whose contributions generalize rather than overfit. In comparison, Oort shows higher variability (e.g., Accuracy 0.6866 and Loss 0.8118), indicating sensitivity to sampling dynamics and seed effects, whereas VARs-FL maintains competitive Precision while improving both F1

scores, demonstrating a balanced reduction in errors rather than a one sided shift in the precision-recall trade-off.

B. Convergence Speed

Table VI shows that VARS-FL converges significantly faster and more reliably than FedAvg, Oort, and PoC across all three seeds, as measured by rounds required to reach fixed accuracy thresholds. At the 75% threshold, VARS-FL is consistently the fastest method, requiring only 16, 20, and 18 rounds for Seeds 7, 42, and 123, corresponding to approximately $\times 1.9$, $\times 1.4$, and $\times 1.8$ speedups versus FedAvg, respectively; it also outpaces PoC in every case (e.g., 16 vs. 20 rounds in Seed 7).

At the 80% threshold, VARS-FL is the only method that *consistently reaches the target* across all seeds, achieving 63, 60, and 58 rounds, while baselines frequently fail to reach 80% within 100 rounds (FedAvg fails in Seeds 42 and 123; Oort fails in all three; PoC reaches the threshold but requires more rounds, e.g. 93 vs. 60 in Seed 42 and 67 vs. 58 in Seed 123).

Overall, these results indicate that VARS-FL not only improves final performance but also accelerates time-to-accuracy and increases robustness to seed variability, particularly at higher-accuracy thresholds where weaker selection strategies tend to stall.

TABLE VI
ROUNDS TO REACH ACCURACY THRESHOLD (DNN, 100 CLIENTS)

Seed	Thresh.	FedAvg	Oort	PoC	VARS-FL	Speedup
7	75%	30	26	20	16	$\times 1.9$ vs. FedAvg
	80%	99	—	99	63	36% fewer rounds
42	75%	27	38	24	20	$\times 1.4$ vs. FedAvg
	80%	—	—	93	60	FedAvg never reaches
123	75%	32	22	29	18	$\times 1.8$ vs. FedAvg
	80%	—	—	67	58	FedAvg/Oort never reach

C. Training Dynamics

Figure 5 shows the test accuracy trajectory across 100 rounds. All methods converge at a similar rate during the cold-start phase (rounds 1–15), after which VARS-FL’s reputation-driven selection takes effect and its accuracy curve separates clearly from the rest. VARS-FL reaches the 80% threshold at round 58, while Power-of-Choice trails at round 67 and both FedAvg and Oort fail to reach this threshold within the 100-round budget (Table VI). Oort exhibits persistent high-amplitude oscillations throughout training, reflecting the instability induced by selecting clients based on local loss under this non-IID partition—rounds where locally-lossy clients are selected pull the global model in directions misaligned with the global objective, causing accuracy to fluctuate rather than converge.

Figure 6 provides the clearest evidence for the objective-alignment argument. From approximately round 20 onward, VARS-FL achieves strictly lower test loss than all baselines, converging to 0.489 by round 100 compared to 0.568 for FedAvg, 0.563 for Power-of-Choice, and 0.778 for Oort. Oort’s loss stagnates well above FedAvg for the majority

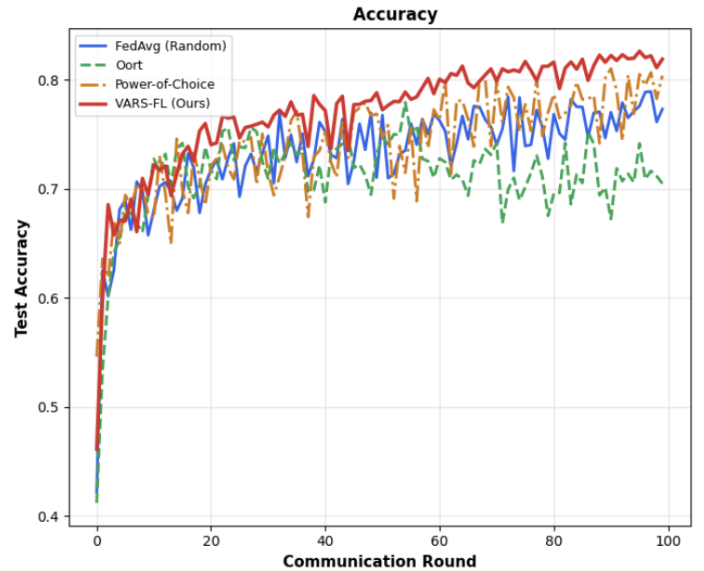


Fig. 5. Test accuracy of all strategies over 100 rounds (100 clients, seed 123)

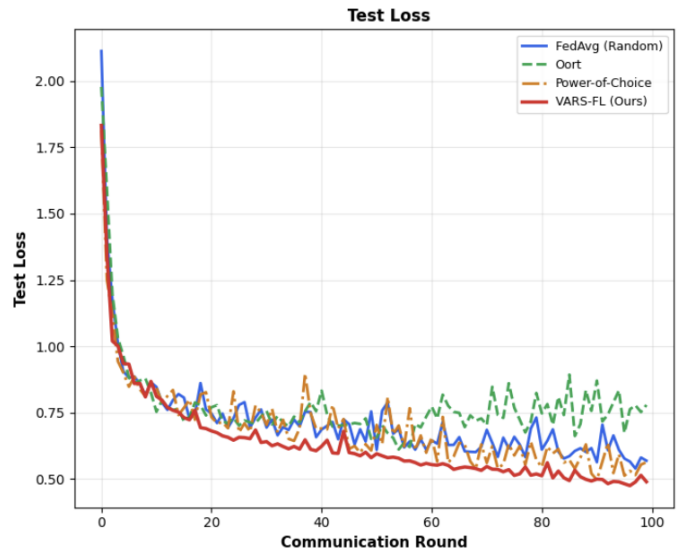


Fig. 6. Test loss of all strategies over 100 rounds (100 clients, seed 123)

of training, confirming that biasing selection toward high local-loss clients not only fails to reduce global loss but can actively impede it. Figure 7 reinforces this conclusion from a relative perspective: VARS-FL’s per-round accuracy delta over FedAvg (red curve) remains predominantly positive across all 100 rounds, demonstrating a sustained rather than episodic advantage. By contrast, Oort’s delta (green) oscillates around zero and trends negative after round 50, indicating that under this seed its local-loss-biased policy provides no reliable improvement over uniform random selection.

D. Per-class recall analysis

Table VII shows that VARS-FL’s gains are concentrated where they matter most: the six classes with FedAvg re-

TABLE V
ALL METHODS AGGREGATED OVER 3 SEEDS (MEAN \pm STD), 100 CLIENTS, 100 ROUNDS

Metric	FedAvg	Oort	PoC	VARS-FL	Δ (VARS-FedAvg)
Accuracy	0.7671 \pm 0.0422	0.6866 \pm 0.1043	0.7925 \pm 0.0204	0.8185 \pm 0.0040	+0.0514 \pm 0.0382
F1-Macro	0.5565 \pm 0.0699	0.5183 \pm 0.0800	0.5928 \pm 0.0446	0.6422 \pm 0.0241	+0.0857 \pm 0.0525
F1-Weighted	0.7502 \pm 0.0442	0.6799 \pm 0.0894	0.7745 \pm 0.0301	0.8086 \pm 0.0080	+0.0584 \pm 0.0369
Precision	0.7281 \pm 0.0365	0.7160 \pm 0.0706	0.7544 \pm 0.0275	0.8026 \pm 0.0392	+0.0745 \pm 0.0227
Loss (\downarrow)	0.5852 \pm 0.0657	0.8118 \pm 0.2257	0.5911 \pm 0.0744	0.4937 \pm 0.0200	-0.0916 \pm 0.0457

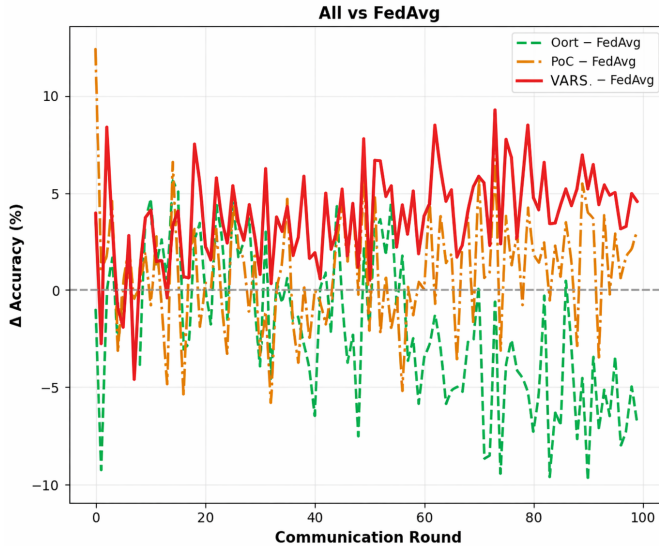


Fig. 7. Per round accuracy delta relative to FedAvg for Oort, PoC, and VARS-FL (100 clients, seed 123)

call below 0.50 all improve under VARS-FL by +0.056 to +0.519 pp, because validation-loss scoring preferentially re-selects the minority-class clients that random sampling reaches too infrequently. Oort achieves even higher recall on some of these classes (e.g. Uploading 0.844) but at catastrophic cost to others (Backdoor: 0.000, DDoS_TCP: 0.156), whereas VARS-FL’s global reward signal prevents such single-class collapse. VARS-FL’s only meaningful regression is Backdoor (−0.110), attributable to clients holding already-well-classified Backdoor data producing small δ_i^t and thus accumulating lower Reputation scores; eight classes remain effectively unchanged ($|\Delta| \leq 0.05$). Overall, VARS-FL’s macro-averaged recall exceeds all baselines across every seed (Table V), confirming that objective-aligned selection distributes recall improvements broadly rather than concentrating gains on a narrow class subset. In particular, the per-class analysis in Table VII shows that VARS-FL strengthens recall on several difficult-to-detect attack types where benchmark selection methods can either underperform or even collapse (e.g., rare or highly heterogeneous classes), indicating that validation-aligned scoring can help surface security attacks that may otherwise be missed.

E. Robustness to Validation Set Composition

Given that VARS-FL relies on a server-side validation set to

TABLE VII
PER-CLASS RECALL: ALL METHODS — 100 CLIENTS, 100 ROUNDS, SEED 42

Attack Type	FedAvg	Oort	PoC	VARS-FL	Δ
Port_Scanning	0.4059	0.9495	0.9501	0.9253	+0.5194
DDoS_HTTP	0.4027	0.7607	0.5843	0.6700	+0.2673
Ransomware	0.3862	0.6644	0.2636	0.6370	+0.2508
Uploading	0.1474	0.8439	0.4592	0.3738	+0.2264
Fingerprinting	0.1000	0.1000	0.1000	0.2267	+0.1267
Password	0.0723	0.0444	0.0146	0.1285	+0.0562
DDoS_UDP	1.0000	0.9693	0.9926	1.0000	+0.0000
MITM	0.3132	0.2308	0.3132	0.3132	+0.0000
Normal	1.0000	0.9993	1.0000	0.9999	-0.0001
DDoS_ICMP	0.9998	0.9940	0.9993	0.9995	-0.0003
SQL_injection	0.9060	0.1025	0.8405	0.9017	-0.0043
XSS	0.0637	0.1290	0.0000	0.0570	-0.0067
Vulnerability_scanner	0.7623	0.7355	0.8487	0.7435	-0.0188
DDoS_TCP	0.9533	0.1557	0.8382	0.9226	-0.0306
Backdoor	0.8965	0.0000	0.9150	0.7868	-0.1097

Δ shows change VARS-FL vs. FedAvg. Rows grouped: top (above first rule) = VARS-FL gain $> +0.05$, middle = $|\Delta| \leq 0.05$, bottom = VARS-FL loss < -0.05 .

compute client scores, we investigate whether the validation-loss improvement signal δ_i^t in Eq. 7 depends on the *composition* of the server-side validation set \mathcal{D}_{val} . Since practical deployments usually have access to a small balanced validation set with a fixed number of attack samples per class collected in a controlled setting, rather than large stratified holdouts, we evaluate VARS-FL under a uniform validation set (equal samples per class) to test the robustness of the selection mechanism.

In this ablation, we modify only the server-side validation set and run VARS-FL on the same three random seeds used in Section V, keeping the test set fixed for both conditions to ensure a fair comparison of downstream performance. The original validation set used in our main experiments is *stratified*, containing 110,407 samples drawn proportionally to the class frequencies of Edge-IIoTset. The *uniform* validation set is considerably smaller at $n = 2,250$ samples (150 per class for all 15 classes), as the per-class count is bounded by the rarest attack (*Fingerprinting*). All other components of the training pipeline—training data, client partitions, model architecture, and hyperparameters—remain unchanged. The contrast in class distribution between the two validation sets is illustrated in Figure 8.

The results of the validation set comparison are reported

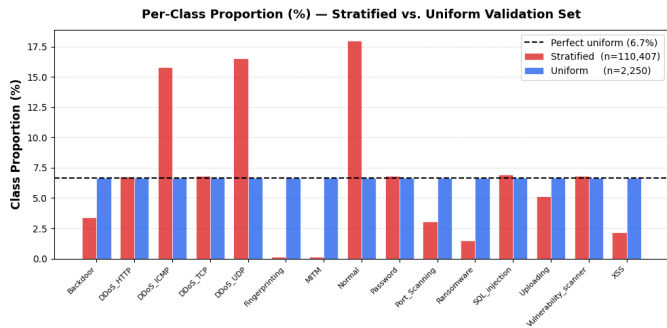


Fig. 8. Class data proportions for the stratified ($n = 110,407$) and uniform ($n = 2,250$) validation sets. The stratified set reflects the natural class imbalance of Edge-IIoTset. The uniform set assigns exactly 150 samples per class and aligns with the perfect-uniform baseline (dashed line at 6.7%).

in Table VIII. The table shows the test-set performance (mean \pm std over three seeds) under both validation set distributions. Between both configurations, all metric results shift by less than one percentage point. The accuracy changes by only 0.24 pp, showing that the overall performance of the model is not significantly affected by the change in validation set composition. Most notably, F1-Macro, being the most likely to degrade if δ_i^t were biased toward majority classes, changes by only 0.48 pp, well within the seed-to-seed standard deviation of ± 2.41 pp observed in our main results. The validation loss shows barely any change ($\Delta = -0.0049$), and variance decreases with the uniform distribution (std drops from 0.0200 to 0.0136). This is consistent with reduced class imbalance noise on the smaller balanced distribution.

TABLE VIII
VARS-FL TEST PERFORMANCE UNDER STRATIFIED VS. UNIFORM VALIDATION SETS USED FOR CLIENT SCORING (3 SEEDS, 100 CLIENTS, 100 ROUNDS). THE TEST SET IS IDENTICAL ACROSS BOTH COLUMNS.

Metric	Stratified Val ($n = 110,407$)	Uniform Val ($n = 2,250$)	Δ
Accuracy	0.8185 \pm 0.0040	0.8161 \pm 0.0071	-0.0024
F1-Macro	0.6422 \pm 0.0241	0.6374 \pm 0.0278	-0.0048
F1-Weighted	0.8086 \pm 0.0080	0.8041 \pm 0.0110	-0.0045
Precision	0.8026 \pm 0.0392	0.7391 \pm 0.0466	-0.0635
Loss (\downarrow)	0.4937 \pm 0.0200	0.4888 \pm 0.0136	-0.0049

The key to this robustness is that the scoring mechanism ranks clients by their *relative* loss improvement for each client and not their absolute loss values. The formulation of δ_i^t itself describes the score as a *difference* of two losses computed on the *same* validation set (the loss before the client’s update and the loss after). Therefore, any distributional bias present in $\mathcal{L}_{\text{val}}(\theta^{t-1})$ also appears in $\mathcal{L}_{\text{val}}(\theta_i^t)$ and largely cancels. Only the *relative* loss improvement of each client remains, which is the signal needed to rank clients. This shows that class distribution of validation set has minimal impact on VARS-FL scoring, as long as it is large enough that loss changes can be reliably detected above sampling noise.

This finding is significant for deployment because it shows that operators do not need to maintain a large stratified validation set that tracks the (often unknown or non-stationary) global attack distribution. This is well-suited for IIoT environments, where the threat landscape evolves over time. Furthermore, the server validation set must be constructed independently from a limited trusted source rather than aggregated from client data, respecting federated learning’s core privacy constraint where clients cannot expose raw data even to the server. These results confirm that VARS-FL is robust to the choice of validation set, as a small class-balanced set of a few thousand samples, collected independently from client devices, is sufficient to drive the selection mechanism reliably. Overall, this strengthens the practical feasibility of VARS-FL for IIoT deployments, where the true class distribution is hard to estimate and data sovereignty requirements prevent the server from accessing client traffic directly

VI. DISCUSSION AND CONCLUSION

We presented VARS-FL, a client selection framework that addresses the limitations of stateless and proxy-based strategies through a validation-aligned, accumulation-based Reputation mechanism. By combining a sliding-window average of recent validation-loss improvements with a logarithmically scaled participation term, VARS-FL captures both short-term utility and long-term reliability, enabling an effective balance between exploration and exploitation while preventing the exclusion of infrequent but informative clients. Defining the selection reward as global validation-loss reduction ensures alignment with the optimization objective, avoiding the misalignment issues inherent to local proxy metrics under non-IID data. Experimental results on a 15-class intrusion detection task show that VARS-FL consistently improves convergence speed, stability, and overall performance, reducing the rounds required to reach target accuracy by up to 36% and achieving lower test loss with minimal cross-seed variance compared to FedAvg, Oort, and Power-of-Choice. A key limitation is the reliance on a server-side validation set; while results demonstrate robustness to class imbalance, sufficient coverage of all classes remains necessary, as unseen classes may be undervalued. Future work will explore coverage-aware scoring, theoretical convergence guarantees, and adaptive reputation mechanisms. Overall, VARS-FL reframes client selection as an objective-aligned, evidence-driven process, providing a principled and practical solution for federated learning under heterogeneous and non-IID data distributions.

ACKNOWLEDGMENT

This work was supported by the United Arab Emirates University under Grant (G00005769).

REFERENCES

- [1] B. McMahan, E. Moore, D. Ramage, S. Hampson, and B. A. y Arcas, “Communication-efficient learning of deep networks from decentralized data,” in *Proceedings of the 20th International Conference on Artificial Intelligence and Statistics (AISTATS)*, 2017, pp. 1273–1282.

- [2] P. Kairouz, H. B. McMahan, B. Avent, A. Bellet, M. Bennis, A. N. Bhagoji, K. Bonawitz, Z. Charles, G. Cormode, R. Cummings *et al.*, “Advances and open problems in federated learning,” *Foundations and Trends in Machine Learning*, vol. 14, no. 1–2, pp. 1–210, 2021.
- [3] M. A. Ferrag, O. Friha, D. Hamouda, L. Maglaras, and H. Janicke, “Edge-iiotset: A new comprehensive realistic cyber security dataset of iot and iiot applications for centralized and federated learning,” *IEEE Access*, vol. 10, pp. 40281–40306, 2022.
- [4] W.-C. Chung, C.-A. Lo, Y.-H. Lin, Z.-H. Chen, and C.-L. Hung, “Decentralized federated learning with non-iid data: Challenges, trends, and future opportunities,” *ACM Computing Surveys*, vol. 58, no. 8, pp. 1–41, 2026.
- [5] D. Hamouda, M. A. Ferrag, N. Benhamida, and H. Seridi, “Ppss: A privacy-preserving secure framework using blockchain-enabled federated deep learning for industrial iiots,” *Pervasive and Mobile Computing*, vol. 88, p. 101738, 2023.
- [6] D. Hamouda, M. A. Ferrag, N. Benhamida, H. Seridi, and M. C. Ghanem, “Revolutionizing intrusion detection in industrial iot with distributed learning and deep generative techniques,” *Internet of Things*, vol. 26, p. 101149, 2024.
- [7] J. Konečný, H. B. McMahan, F. X. Yu, P. Richtárik, A. T. Suresh, and D. Bacon, “Federated learning: Strategies for improving communication efficiency,” in *NIPS Workshop on Private Multi-Party Machine Learning*, 2016.
- [8] K. Bonawitz, V. Ivanov, B. Kreuter, A. Marcedone, H. B. McMahan, S. Patel, D. Ramage, A. Segal, and K. Seth, “Practical secure aggregation for privacy-preserving machine learning,” in *Proceedings of the ACM SIGSAC Conference on Computer and Communications Security (CCS)*, 2017.
- [9] D. Alistarh, J. Grubic, J. Li, R. Tomioka, and M. Vojnovic, “QSGD: Communication-efficient SGD via gradient quantization and encoding,” in *Advances in Neural Information Processing Systems (NeurIPS)*, 2017.
- [10] A. F. Aji and K. Heafield, “Sparse communication for distributed gradient descent,” in *Proceedings of the Conference on Empirical Methods in Natural Language Processing (EMNLP)*, 2017.
- [11] T. Nishio and R. Yonetani, “Client selection for federated learning with heterogeneous resources in mobile edge,” in *Proceedings of the IEEE International Conference on Communications (ICC)*, 2019, pp. 1–7.
- [12] W. Shi, S. Zhou, Z. Niu, M. Jiang, and L. Geng, “Joint device scheduling and resource allocation for latency constrained federated learning,” *IEEE Transactions on Wireless Communications*, vol. 20, no. 1, pp. 453–467, 2021.
- [13] M. K. Quan, P. N. Pathirana, M. Wijayasundara, S. Setunge, D. C. Nguyen, C. G. Brinton, D. J. Love, and H. V. Poor, “Federated learning for cyber physical systems: a comprehensive survey,” *IEEE Communications Surveys & Tutorials*, 2025.
- [14] K. Pfeiffer, M. Rapp, R. Khalili, and J. Henkel, “Federated learning for computationally constrained heterogeneous devices: A survey,” *ACM Computing Surveys*, vol. 55, no. 14s, pp. 1–27, 2023.
- [15] M. P. Uddin, Y. Xiang, M. Hasan, J. Bai, Y. Zhao, and L. Gao, “A systematic literature review of robust federated learning: Issues, solutions, and future research directions,” *ACM Computing Surveys*, vol. 57, no. 10, pp. 1–62, 2025.
- [16] L. Fu, H. Zhang, G. Gao, M. Zhang, and X. Liu, “Client selection in federated learning: Principles, challenges, and opportunities,” *IEEE Internet of Things Journal*, vol. 10, no. 24, pp. 21811–21819, 2023.
- [17] D. Thakur, A. Guzzo, G. Fortino, and F. Piccialli, “Green federated learning: A new era of green aware ai,” *ACM Computing Surveys*, vol. 57, no. 8, pp. 1–36, 2025.
- [18] N. Benarba and S. Bouchenak, “Bias in federated learning: A comprehensive survey,” *ACM Computing Surveys*, vol. 57, no. 11, pp. 1–36, 2025.
- [19] M. Ye, X. Fang, B. Du, P. C. Yuen, and D. Tao, “Heterogeneous federated learning: State-of-the-art and research challenges,” *ACM Computing Surveys*, vol. 56, no. 3, pp. 1–44, 2023.
- [20] O. R. A. Almanifi, C.-O. Chow, M.-L. Tham, J. H. Chuah, and J. Kanesan, “Communication and computation efficiency in federated learning: A survey,” *Internet of Things*, vol. 22, p. 100742, 2023.
- [21] F. Lai, X. Zhu, H. V. Madhyastha, and M. Chowdhury, “Oort: Efficient federated learning via guided participant selection,” in *Proceedings of the 15th USENIX Symposium on Operating Systems Design and Implementation (OSDI)*, 2021, pp. 19–35.
- [22] E. T. M. Beltrán, M. Q. Pérez, P. M. S. Sánchez, S. L. Bernal, G. Bovet, M. G. Pérez, G. M. Pérez, and A. H. Celdrán, “Decentralized federated learning: Fundamentals, state of the art, frameworks, trends, and challenges,” *IEEE Communications Surveys & Tutorials*, vol. 25, no. 4, pp. 2983–3013, 2023.
- [23] T. Li, A. K. Sahu, M. Zaheer, M. Sanjabi, A. Talwalkar, and V. Smith, “Federated optimization in heterogeneous networks,” in *Proceedings of Machine Learning and Systems (MLSys)*, 2020.
- [24] Y. Jee Cho, J. Wang, and G. Joshi, “Towards understanding biased client selection in federated learning,” in *Proceedings of The 25th International Conference on Artificial Intelligence and Statistics*, ser. Proceedings of Machine Learning Research, vol. 151. PMLR, 2022, pp. 10351–10375.
- [25] J. Goetz, K. Malik, D. Bui, S. Moon, H. Liu, and A. Kumar, “Active federated learning,” *arXiv preprint arXiv:1909.12641*, 2019.
- [26] M. Tang, X. Ning, Y. Wang, J. Sun, Y. Wang, H. Li, and C. Yao, “Fed-Cor: Correlation-based active client selection strategy for heterogeneous federated learning,” in *Proceedings of the IEEE/CVF Conference on Computer Vision and Pattern Recognition (CVPR)*, 2022, pp. 10102–10111.
- [27] X. Cao, M. Fang, J. Liu, and N. Z. Gong, “FLTrust: Byzantine-robust federated learning via trust bootstrapping,” in *Proceedings of the Network and Distributed System Security Symposium (NDSS)*, 2021.
- [28] X. Li, K. Huang, W. Yang, S. Wang, and Z. Zhang, “On the convergence of FedAvg on non-IID data,” in *International Conference on Learning Representations (ICLR)*, 2020.
- [29] S. P. Karimireddy, S. Kale, M. Mohri, S. J. Reddi, S. Stich, and A. T. Suresh, “SCAFFOLD: Stochastic controlled averaging for federated learning,” in *Proceedings of the International Conference on Machine Learning (ICML)*, 2020, pp. 5132–5143.
- [30] Q. Li, B. He, and D. Song, “Model-contrastive federated learning,” in *Proceedings of the IEEE/CVF Conference on Computer Vision and Pattern Recognition (CVPR)*, 2021, pp. 10713–10722.
- [31] F. Lai, Y. Dai, S. Singapuram, J. Liu, X. Zhu, H. V. Madhyastha, and M. Chowdhury, “FedScale: Benchmarking model and system performance of federated learning at scale,” in *Proceedings of the International Conference on Machine Learning (ICML)*, 2022, pp. 11814–11827.
- [32] P. Blanchard, E. M. El Mhamdi, R. Guerraoui, and J. Stainer, “Machine learning with adversaries: Byzantine tolerant gradient descent,” in *Advances in Neural Information Processing Systems (NeurIPS)*, 2017, pp. 119–129.
- [33] E. M. El Mhamdi, R. Guerraoui, and S. Rouault, “The hidden vulnerability of distributed learning in Byzantium,” in *Proceedings of the International Conference on Machine Learning (ICML)*, 2018, pp. 3521–3530.
- [34] L. Collins, H. Hassani, A. Mokhtari, and S. Shakkottai, “Exploiting shared representations for personalized federated learning,” in *Proceedings of the International Conference on Machine Learning (ICML)*, 2021, pp. 2089–2099.
- [35] C. T. Dinh, N. H. Tran, and T. D. Nguyen, “Personalized federated learning with Moreau envelopes,” in *Advances in Neural Information Processing Systems (NeurIPS)*, 2020, pp. 21394–21405.
- [36] A. Garivier and É. Moulines, “On upper-confidence bound policies for switching bandit problems,” in *Proceedings of the International Conference on Algorithmic Learning Theory (ALT)*, 2011, pp. 174–188.
- [37] D. J. Russo, B. Van Roy, A. Kazerouni, I. Osband, and Z. Wen, “A tutorial on Thompson sampling,” *Foundations and Trends in Machine Learning*, vol. 11, no. 1, pp. 1–96, 2018.
- [38] V. Motukuri, R. M. Parizi, S. Pouriyeh, Y. Huang, A. Dehghantanha, and G. Srivastava, “A survey on security and privacy of federated learning,” *Future Generation Computer Systems*, vol. 115, pp. 619–640, 2021.
- [39] T. D. Nguyen, S. Marchal, M. Miettinen, H. Fereidooni, N. Asokan, and A.-R. Sadeghi, “DfIoT: A federated self-learning anomaly detection system for iot,” in *IEEE International Conference on Distributed Computing Systems (ICDCS)*, 2019.
- [40] V. Rey, P. M. Sanchez Sanchez, A. H. Celdrán, and G. Bovet, “Federated learning for malware detection in IoT devices,” *Computer Networks*, vol. 204, p. 108693, 2022.
- [41] S. T. Rahman, A. Mansoor, M. Shamim Hossain, and M. M. Rahman, “Internet of things intrusion detection: Centralized, on-device, or federated learning?” *IEEE Network*, vol. 34, no. 6, pp. 310–317, 2020.
- [42] I. Sharafaldin, A. H. Lashkari, and A. A. Ghorbani, “Toward generating a new intrusion detection dataset and intrusion traffic characterization,” in *Proceedings of the 4th International Conference on Information Systems Security and Privacy (ICISSP)*, 2018, pp. 108–116.

- [43] N. Moustafa, "A new distributed architecture for evaluating AI-based security systems at the edge: Network TON_IoT datasets," *Sustainable Cities and Society*, vol. 72, p. 102994, 2021.
- [44] Y. Meidan, M. Bohadana, Y. Mathov, Y. Mirsky, A. Shabtai, D. Breitenbacher, and Y. Elovici, "N-BaIoT: Network-based detection of IoT botnet attacks using deep autoencoders," *IEEE Pervasive Computing*, vol. 17, no. 3, pp. 12–22, 2018.